

Dimensional Effect of Doped Porous Ge Using SILVACO TCAD Simulation for Potential Optoelectronics Application

A.F. Abd Rahim^{1,*}, N. S. I. Mohamad Shuhaimi², N. S. Mohd Razal³, R. Radzali⁴, A. Mahmood⁵, I.H. Hamzah⁶, M F Packer Mohamed⁷

^{1,2,3,4,6}Faculty of Electrical Engineering, Universiti Teknologi MARA, Cawangan Pulau Pinang, 13500 Permatang Pauh, Pulau Pinang, Malaysia

⁵Department of Applied Sciences, Universiti Teknologi MARA, Cawangan Pulau Pinang, 13500 Permatang Pauh, Pulau Pinang, Malaysia

⁷School of Electrical and Electronic Engineering, Engineering Campus, Universiti Sains Malaysia, 14300 Nibong Tebal, Penang, Malaysia

*corresponding author: ¹alhan570@uitm.edu.my

ARTICLE HISTORY

ABSTRACT

Received
27 May 2021

Accepted
16 July 2021

Available online
12 August 2021

Ge is considered to have several advantages over Si due to its high mobility and direct bandgap, which makes it ideal for optoelectronic applications. The manipulation of bulk Ge into small structures has drawn a lot of interest due to the numerous distinctive properties caused by the impact of size quantization. Porous materials are ideally suited for sensing application due to their large effective surface area beside the fabrication of porous is simple. In this work, porous Ge is investigated for potential visible to near-infrared metal semiconductor metal (MSM) photodetector. The study investigated the performance and characterization of porous Ge (P-Ge) on Si substrate at different depths of porous (1 μm , 0.25 μm and 0.01 μm) by using SILVACO Athena and Atlas device simulator. Athena process simulator was used to construct the device structure while ATLAS device simulator was used to characterize the electrical and optical characteristics' effect on the different sizes of the P-Ge fabricated on the Si substrate. The comparison of the porous devices were then made with bulk Ge devices (bulk Ge-on-Si, bulk Ge-on-Ge) to identify the exploitation of porosity resulted in a significant performance of current gains, spectral response, Schottky barrier height, and also photo and dark current. It was found that the P-Ge at 0.01 μm depth showed an improved current gain compared to other porous structures while bulk Ge-on-Si obtain greater current gain than bulk Ge-on-Ge. This evidence indicates that P-Ge produces a better performance of MSM photodetector than the bulk device. The spectral response of P-Ge shows a peak response at 800nm, which is the near-infrared (IR) region supporting the feasibility of the P-Ge to be utilized for visible to near IR photodetection.

Keywords: Geon Si; Ge porous; MSM Photodetector; Spectral response;TCAD.

1. INTRODUCTION

Recently, high-tech applications such as fibre optic telecommunications, optical interconnect on chips, and CMOS imaging cameras need an efficient photodetection of visible and near-infrared light [1]. Photodetectors in the current market have been fabricated using various materials, for example bulk semiconductors such as silicon (Si), germanium (Ge), and indium gallium arsenide (InGaAs) since those materials have a huge impact on the wavelength

detection range. Ge is said to have several advantages over Si due to its high mobility and direct bandgap that promising its ideality for optoelectronic fabrication. There is such a high attentiveness toward quantum dots Ge-on-Si heterostructures due to the number of their unique properties caused by the effects of size quantization. Porous materials are ideally suited for sensing application due to their large effective surface area beside the fabrication of porous. It is easy to be controlled because of highly definable parameters such as porosity and refractive index[2]. On the other hand, a researcher found that porosity, pore diameter, and depth of porous layer can be affected by several factors such as type of the substrate and dopant, current density, and the electrolyte concentration[3].

The compatibility of Ge substitution with Si technology and its ability in self-assembled porous Ge has supported efficient work in this study. One of the studies shows that the typical responsivity of 10 μm long integrated Ge-on-Si photodetector is 1A/W at $1.55\ \mu\text{m}$ wavelength, which is greater than the typical responsivity of Si photodetector [4]. In addition, a study has been conducted to compare the epitaxial Ge-on-Ge and epitaxial Ge-on-Si and tested on Ge-on-Glass (GOG) fabricated by layer transfer. It shows that Ge-on-Ge exhibited very low dark currents with average current densities of $100\ \mu\text{A}/\text{cm}^2$, while epitaxial Ge-on-Si shows current densities twenty times larger, even if the measured $2\text{mA}/\text{cm}^2$ is among the lowest ever reported dark current densities for Ge-on-Si photodetector [5]. In other work, nanoporous Ge is highly potential for infrared photodetection since the significant absorption spectrum is beyond $1300\ \text{nm}$ [6]. Photodetector with excellent performance and monolithic integration with Si CMOS for potential visible MSM has been demonstrated by Abd. Rahim et. al. The work proves that porous SiGe exhibits a higher energy band gap and greater current gain as compared to bulk Ge. Furthermore, the finding of spectral response is at $590\ \text{nm}$, which is a visible wavelength [7]. Si is chosen as the substrate in mostly existing technology since it is compatible as a good substrate.

This has motivated the need for porous germanium study to observe and analyze the optical performance of bulk and porous germanium towards the infrared spectrum. A detailed comparison shows the superior performance of germanium as it has a potential for application in photonics and high-speed device in conjunction with its high carrier mobility and unique optical properties at the nanoscale [8]. In this work, the SILVACO TCAD tool has been used to simulate semiconductor device fabrication. The work done by Zaimah et. al. shows that SILVACO TCAD can obtain optimum device performance for better device fabrication [9]. Different sizes of porous Ge-on-Si and bulk Ge were presented in this research and the devices were tested for potential visible to near-IR MSM photodetector. Finally, the comparison based on electrical and optical characteristics has been evaluated when several parameters of the structure are varied.

2. METHODOLOGY

This research starts with the construction of the device structure on SILVACO TCAD tools. There are five different types of structures constructed. The structures have been varied in terms of their pore depths with a fixed pore diameter of $1\ \mu\text{m}$. Table 1 shows the tabulation of the structure depths and diameters, while Figure 1 shows the flowchart of the process simulation to produce the output of the simulation.

Table 1: Size of bulk Ge-on-Si, bulk Ge-on-Ge and different depths of porous Ge-on-Si

Structure	Depth of porous (μm)	Diameter of porous (μm)
Bulk Ge-on-Si	-	-
Bulk Ge-on-Ge	-	-
Porous Ge-on-Si	0.01	1.00
	0.25	
	1.00	

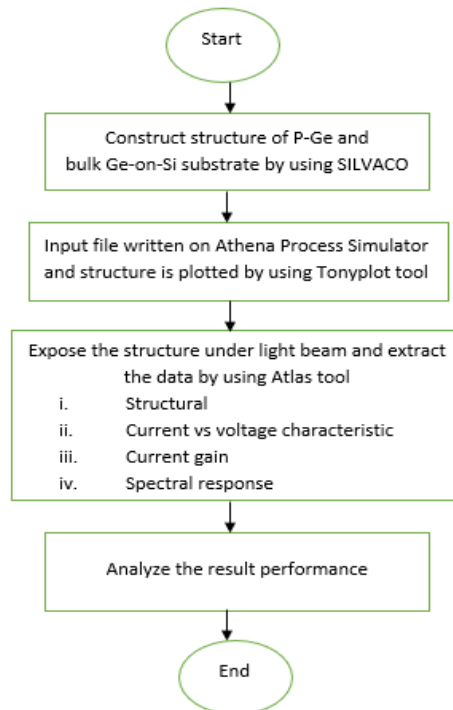


Figure 1: Flowchart for simulation of bulk Ge and porous germanium on silicon by using Athena and Atlas simulator.

To obtain the output of electrical and optical characteristics for each structure, several commands or statements need to be set on the Atlas simulator. Table 2 shows the statements that have been used in the device simulation setting.

Table 2: Atlas commands and purpose of each command

Command or statement	Purpose
Mesh, Region, Electrode, Doping	Specification of structure
Material, Models, Contact, Interface	Specification of material model
Method	Numerical method selection
Log, Solve, Load, Save	Solution Specification
Tonyplot	Result analysis

The five structures were constructed firstly by using Athena Process Simulator before proceeding with the device simulation using Atlas. Germanium and silicon have been defined as the substrates for bulk Ge-on-Ge and Ge-on-Si structures, respectively. The substrates were first initialized, and the mesh was defined by setting up the value of x and y-axis gridlines for all the structures. In this study, the thickness and porosity of the Ge layer are varied as stated in Table 1. A Ge layer was deposited on the Si substrate before conducting the etching process to form the porous structures. The structure is a mirror at the right side and finally, the contact of aluminium is formed at the edges of the structure to set cathode and anode electrode. A light source had been applied by defining the beam power and its respective wavelength to get the photoresponse of the devices. Figure 2 shows a schematic diagram of the fabrication process.

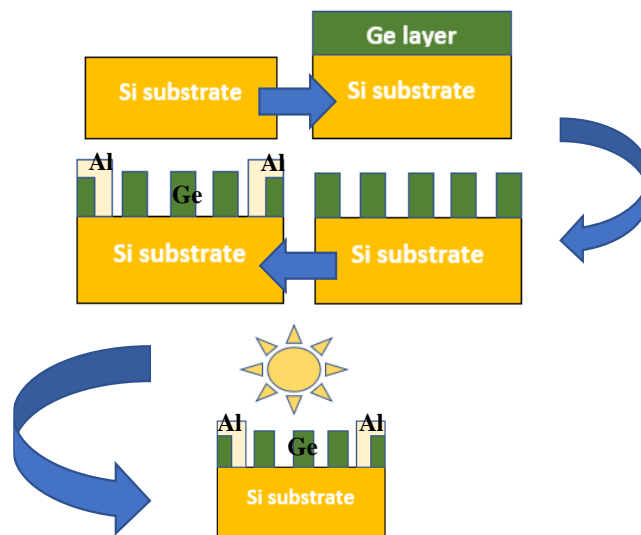


Figure 2: Schematic diagram showing the simulation process flow of P-Ge-on-Si substrate

Figure 3 shows the setting of the mesh or grid lines for the device. The photodetector's electrical and optical characteristics can be accurately simulated by forming a fine mesh at the device's active region. The setting of the mesh is by defining the location of the x and y-axis with their respective spacing as shown in Figure 4.

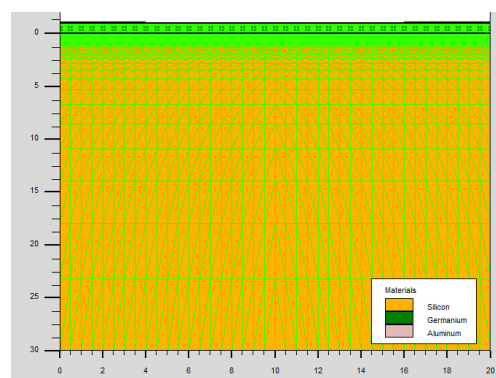


Figure 3: Mesh definition for bulk Ge-on-Si

```
go athena
line x loc=0.00 spac=0.50
line x loc=10.00 spac=0.50
line y loc=0.00 spac=0.05
line y loc=0.25 spac=0.02
line y loc=1.00 spac=0.10
line y loc=30.00 spac=10.00
```

Figure 4: Mesh setting command

The setting of structure is 20 μm width x 30 μm length. P-N junction of the device was formed by implanted with phosphorus doping of $1 \times 10^{14} \text{ cm}^{-3}$ and boron doping of $1 \times 10^{17} \text{ cm}^{-3}$. The implantation process was followed by the drive-in of 1000°C for 50 minutes. Next, the wafer was subjected to deposit a contact and electrode statement to form MSM photodetector. Aluminium (Al) has been chosen as a contact for this device. The command is written as follows describe in Figure 5.

```
deposit germanium thick=0.25
deposit aluminium thick=0.10 division=3
etch aluminium right pl.x=4
struct mirror right
electrode name=anode x=2.00
electrode name=cathode x=18.00
```

Figure 5: Depositing Aluminum contact electrode

The three porous structures of this study need to undergo the etching process of the germanium layer at a specific coordinate. Etching work is textured according to the thickness of germanium on top of the silicon substrate. Figure 6 shows the command of the etching process written on Athena as follows for P-Ge with a pore diameter of 0.25 μm .

```
etch germanium start x=1.00 y=-0.25
etch cont x=1.50 y=-0.25
etch cont x=1.50 y=-0.25
etch done x=1.00 y=0.00
```

Figure 6: Command to set the etching process to form P-Ge.

Then, the simulation is continued with the Atlas device simulator to set up the material and physical model of the input file. Among the physical properties and models that exist in this tool such as recombination, photogeneration, mobility and lifetime, this study uses the Auger recombination model as the physical model and the command written as shown in Figure 7 below.

```
physical models  
models conmob fldmob srh auger print
```

Figure 7: Physical models setting

Besides, the photodetection of the structures was analyzed by defining the beam power of the light source on top of the device. This will generate the spectral response output and I-V characteristics of the device. The spectral response shows the responsivity of the device over the range of the wavelength. The biasing and solution of specification group setup that solve the spectral response and I-V characteristics are shown in Figure 8.

```
beam num=1 x.origin=10.00 y.origin=-1.0 angle=90.0  
power.file=optoex02.spec wae1.end=0.8 wave1.num=5  
  
method newton trap  
  
solve init  
  
log outfile=I-Vlight.log  
  
solve b1=750 vanode=0.0 vstep=0.1 vfinal=5.0  
name=anode  
  
tonyplot I-Vdark.log -overlay I-Vlight.log -set I-Vlight.set
```

Figure 8: Biasing condition setup for spectral response and I-V characteristics

Finally, the current-voltage (I-V) characteristic was obtained from the simulation; hence, evaluation of photodetection performance has been made by extracting the current gain (I_{photo}/I_{dark}) and the spectral response.

3. RESULTS AND DISCUSSION

3.1. Structural characteristics of bulk Ge, p-Ge on Si substrate and bulk Ge on Ge substrate

This device was constructed from several materials before starting the simulation. The materials involved are presented in Figure 9. Figure 10 shows the five structures constructed in this study with the structure of P-Ge of 1 μm being enlarged to show the pore depth.

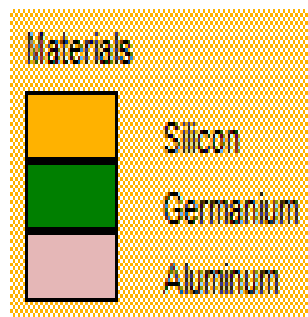


Figure 9: Label notation of region and material of the structure

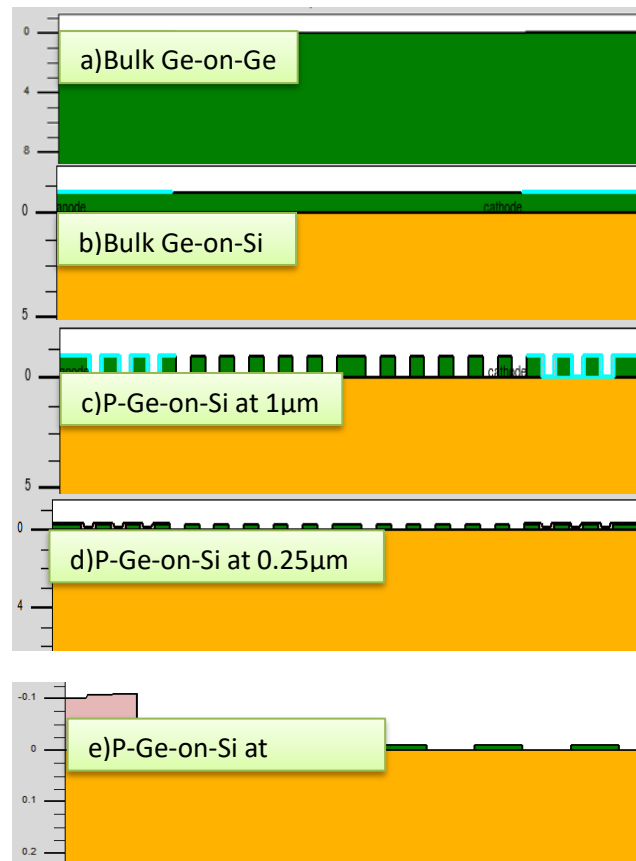


Figure 10: Final structures for a) Bulk Ge-on-Ge, b) Bulk Ge-on-Si, c) P-Ge at 1 μm , depth), d) P-Ge at 0.25 μm depth and e) P-Ge at 0.01 μm depth on Si substrates (enlarged to show the pore depth).

3.2. I-V Characteristics

The current-voltage (I-V) characteristic of a photodetector with no incident light is similar to a rectifying diode [10]. This means that the forward bias will cause an exponential increase in the current, while reverse bias will contribute to a reverse saturation of current. The potential of the structures for photonic application can be observed based on the results of the dark and photocurrent of the devices. Figure 11 presents the dark and photocurrent for the bulk Ge-on-Ge and Ge-on-Si devices. It can be seen that the dark current for bulk Ge-on-Ge at a forward-biased 5 V is slightly lower than the dark current for bulk Ge-on-Si at the same forward-biased voltage. Meanwhile, the photocurrent for both bulk Ge-on-Ge and Ge-on-Si increases with bias voltage before it is saturated as the voltage reaches 0.5 and 1 V, respectively. Figure 12 shows the current-voltage characteristic of P-Ge at different pores depths. Pore depth of 0.01 μm has shown the greatest photocurrent and lowest dark current compared to other pore depths. The trend of the current of the P-Ge structures supports well with the study by Xia et. al. that a slight difference in Ge thickness could be attributed to the optical constant difference of this device [11]. A positive correlation can be seen in Figure 11 and 12 where the photocurrents of all devices are higher than the dark current indicating significant photoresponse of the devices especially the P-Ge samples.

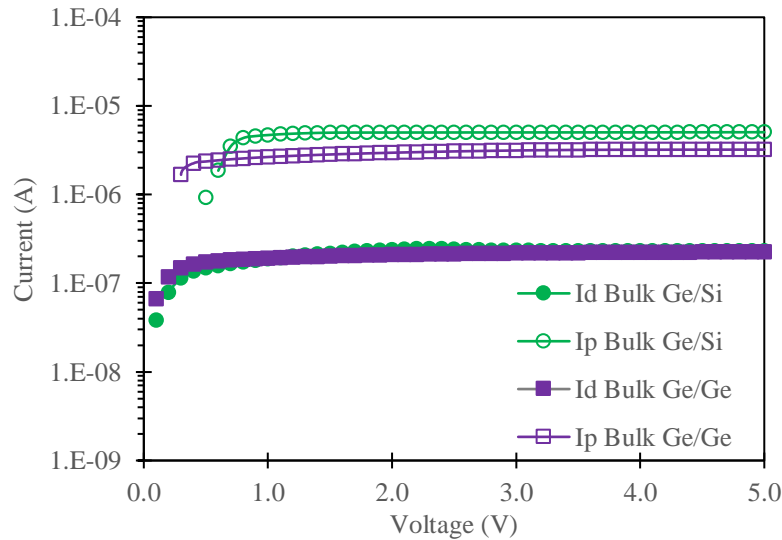


Figure 11: I-V Characteristics of bulk Ge on Si and bulk Ge on Ge substrates.

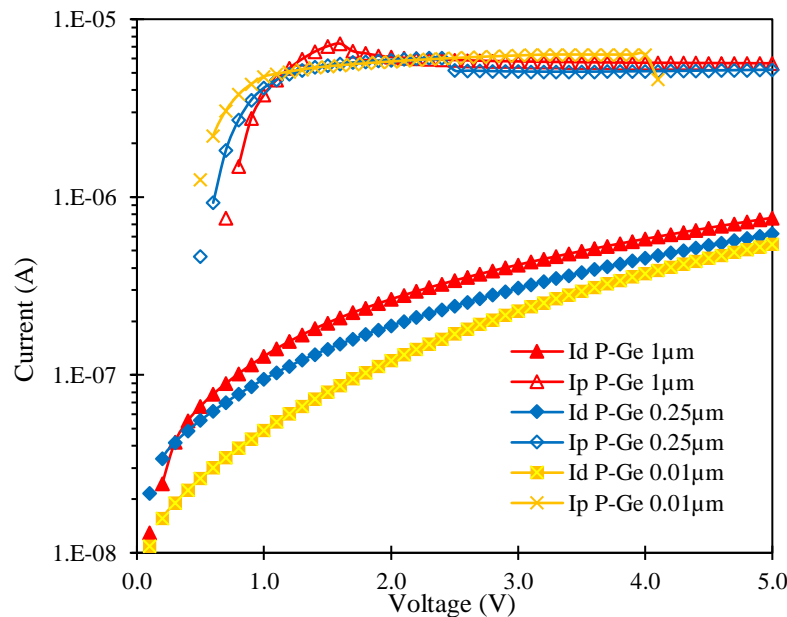


Figure 12: I-V Characteristics of P-Ge on Si with various pores depth.

3.3. Gain (I_p/I_d)

Among the parameters, which define the characteristics of a photodetector, are the response coefficient, the gain, the quantum efficiency, the bandwidth, and the detectivity[11]. In this study, further analysis can be made by finding the ratio of the photocurrent to dark current which is equivalent to the current gain of this device. This result is presented in Figure 13 showing that the P-Ge samples obtain higher current gain compared to bulk Ge. It is believed that the greater photoresponse is attributed to the optical phonon confinement of low dimensional P-Ge than the bulk Ge. The most striking result to emerge from the data is: the lower the depth of the P-Ge (0.01 μm), the greater the current gain. The increment is not only

by the enhancement of the photocurrents but also by the performance of the MSM photodetector.

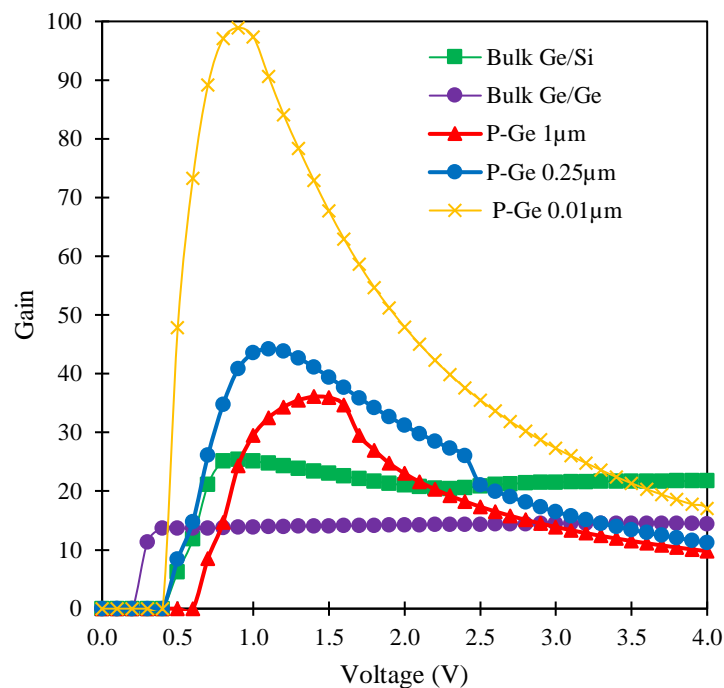


Figure 13: Current gain for bulk Ge and P-Ge devices.

3.4. Schottky Barrier Height

The quality of the Schottky contacts has a big impact on the MSM photodetector performance. The MSM photodetector is made up of two Schottky contacts that are coupled back-to-back. One of the Schottky contacts is forward-biased and the other is reverse-biased when a bias is introduced. To further analyze the I-V characteristics of the devices, the Schottky barrier height (SBH) and ideality factor of the device are extracted. Table 3 presents the parameters extraction of the MSM photodetector for the five samples.

It was observed that the dark current of the P-Ge samples is lower than the bulk Ge samples. The lowest dark current in the P-Ge of 0.01 μm sample can be attributed to the high barrier height (0.5786 eV) of the metal contact. However, the ideality factors for the P-Ge samples show inconsistency as the pore depth increases. This may be ascribed to the barrier inhomogeneities from the metal-semiconductor interface. However, the lower ideality factors indicate the better quality of the Schottky's contacts under investigation for the P-Ge samples as compared to bulk Ge. In addition, the lower dark current of the P-Ge samples may be attributed to the higher resistance of the porous surface experienced in the devices. It is interesting to note that the lower dark current and higher photocurrent of the P-Ge devices resulted in enhanced photocurrent gain of the devices with P-Ge of 0.01 μm exhibited about a factor of four times gain increase compared to bulk Ge-on-Si device at 1V biased. Each of P-Ge device shows terrific response, which produces significant free carriers for enhanced current conduction compared to bulk Ge structure.

Table 3: Comparison of parameter extraction of bulk Ge-on-Si, bulk Ge-on-Ge, and P-Ge devices.

Device	SBH (eV)	Ideality Factor (n)	Id at 1V (A)	Ip at 1V (A)	Gain at 1V
Bulk Ge-on-Si	0.5203	10.22	1.87E-07	4.69E-06	25.11
Bulk Ge-on-Ge	0.5165	22.82	1.91E-07	2.65E-06	13.89
P-Ge 1 μm	0.5601	15.64	1.27E-07	3.76E-06	29.51
P-Ge 0.25 μm	0.5634	8.60	9.46E-08	4.12E-06	43.53
P-Ge 0.01 μm	0.5786	10.92	4.89E-08	4.76E-06	97.35

3.5. Spectral Response

Figure 14 shows the spectral response of the five samples spanning from deep UV to near-infrared regions. The graph is an evidence that the thickness of Ge or pore depth can enhance the spectral response at a specific wavelength. It can be seen that P-Ge samples exhibited enhanced photoresponses as the pore depth increases while the bulk samples showed lower photoresponse as the substrate changes. Based on Figure 14 it is shown that manipulation of the depth of the pores has a significant effect on the spectral response of the structure, with the peak current showing a significant change upon light exposure. Specifically, the P-Ge of 1 μm , exhibited peak current at 810 nm ($E_g=1.53$ eV), while for P-Ge of 0.25 μm and 0.01 μm , the peak currents emerged at 800 nm ($E_g=1.55$ eV), respectively. It has shown that P-Ge exhibits a broader and enhanced photoresponse spanning from the visible region to the near-infrared region (400-1000 nm). The trend following the work by Siantos et.al which shows that, the Ge quantum dot photodetectors fabricated on Si and Ge substrates display improved room-temperature responsivity from visible to near-IR range due to high internal photoconductive gain [1].

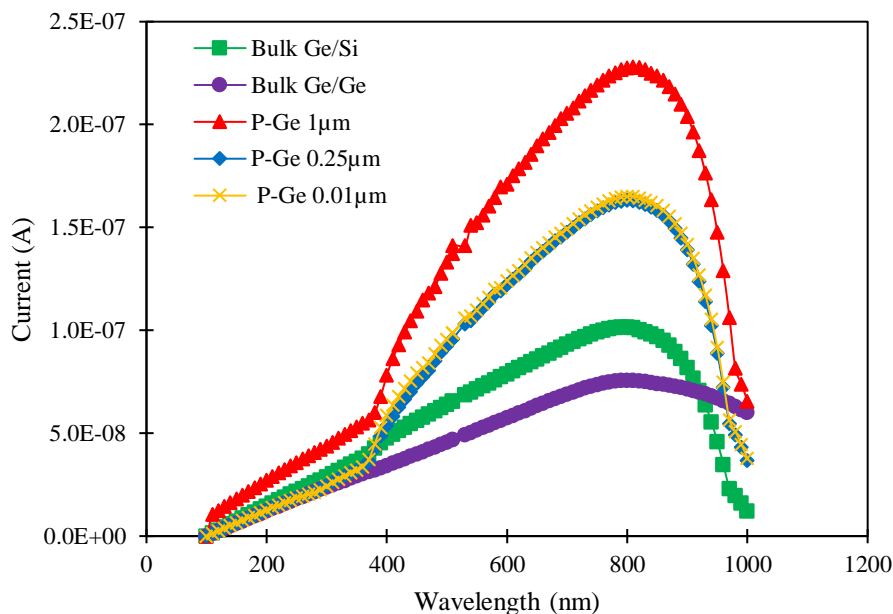


Figure 14: Spectral response of bulk Ge and P-Ge devices.

4. CONCLUSION

The simulation and characterization of bulk Ge and P-Ge for potential MSM photodetectors are carried out successfully by using Silvaco TCAD tools. It is shown that the P-Ge devices produce enhanced photocurrent and lower dark current compared to bulk Ge devices. The manipulation of the pore depth changes the current gain and also the spectra response of the devices. The P-Ge devices show promise for a high-performance photodetector in the visible to near IR region.

ACKNOWLEDGEMENT

The author wishes to thank the members of Digital System Laboratory, Universiti Teknologi MARA Cawangan Pulau Pinang, for the endless technical assistance in this project. The financial support from Universiti Teknologi MARA Cawangan Pulau Pinang is gratefully acknowledged.

REFERENCES

- [1] S. Siontas, D. Li, H. Wang, A. A.V.P.S, A. Zaslavsky, and D. Pacifici, "High-performance germanium quantum dot photodetectors in the visible and near infrared," *Mater. Sci. Semicond. Process.*, vol. 92, pp. 19-27, 2018.
- [2] T. Hutter, G. Wellio, J. Chan, A. V. Kellarev, S. R. Elliott, and S. Ruschin, "Optical Layout for the Measurement of a Porous Silicon Sensor Array," *2017 European Conference on Lasers and Electro-Optics and European Quantum Electronics Conference, Optical Society of America*, paper CH_9_5, 2017
- [3] L. Currano, W. Churaman and C. Becker, "Nanoporous silicon as a bulk energetic material," *TRANSDUCERS 2009 - 2009 International Solid-State Sensors, Actuators and Microsystems Conference*, pp. 2172-2175, 2009.
- [4] L. Vivien et al., "Germanium photodetector integrated in a Silicon-On-Insulator microwaveguide," *2007 4th IEEE International Conference on Group IV Photonics*, pp. 1-3, 2007.
- [5] V. Sorianello et al., "Germanium on insulator near-infrared photodetectors fabricated by layer transfer," *Thin Solid Films*, vol. 518, no. 9, pp. 2501–2504, 2010.
- [6] E. M. Sanehira, C. Tu and L. Y. Lin, "Solution-processed photodetectors using colloidal germanium nanoparticles," *IEEE Photonics Conference 2012*, pp. 386-387, 2012.
- [7] Alhan Farhanah Abd Rahim, Nur'Amirah Zainal Badri, Rosfariza Radzali, Ainorkhilah Mahmood, "Study of low dimensional SiGe island on Si for potential visible Metal-Semiconductor-Metal photodetector", *EPJ Web Conf.*, vol. 162, no. 01062, pp. 1-6, 2017.
- [8] A.F. Abd Rahim, M.R. Hashim, N.K. Ali, A.M. Hashim, M. Rusop, M.H. Abdullah, "The evolution of Si-capped Ge islands on Si (100) by RF magnetron sputtering and rapid thermal processing: The role of annealing times", *Microelectronic Engineering*, vol. 126, pp 134-142, 2014.
- [9] N. Z. Baharom, A. Farhanah, A. Rahim, and A. S. Baharom, "Study of Low Dimensional Ge Island on Si for Visible Metal-Semiconductor-Metal Photodetector," *ESTEEM Academic Journal*, vol. 14 pp. 1–11, 2018.
- [10] OSI optoelectronics, "Photodiode Characteristics and Application," *OSI Optoelectron Application notes*, pp. 1-6, 2009.
- [11] Z. Xia et al., "Single-crystalline germanium nanomembrane photodetectors on foreign nanocavities," *Science Advances*, vol. 3, no. 7, pp. 1–8, 2017.
- [12] F. Omnes, , "Introduction to Semiconductor Photodetectors", pp. 1–14, 2009, <https://doi.org/10.1002/9780470611630.ch1>.